State Prediction of Human-in-the-Loop Multi-rotor System with Stochastic Human Behavior Model ⋆

Joonwon Choi * **Sooyung Byeon** * **Inseok Hwang** *

* *Purdue University, West Lafayette, IN 47907 USA*
(e-mail: {choi774, sbyeon, ihwang}@purdue.edu).

Abstract: Reachability analysis is a widely used method to analyze the safety of a Human-in-the-Loop Cyber Physical System (HiLCPS). It allows the HiLCPS to respond against an imminent threat in advance by predicting reachable states of the system. However, it could lead to an unnecessarily conservative reachable set if the prediction only relies on the system dynamics without explicitly considering human behavior, and thus the risk might be overestimated. To avoid the conservativeness, we present a state probability distribution function (pdf) prediction method which takes into account a stochastic human behavior model represented as a Gaussian Mixture Model (GMM). In this paper, we focus on the multi-rotor controlled by a human operator in a near-collision situation. The stochastic human behavior model is trained using experimental data to represent the human operators' evasive maneuver. Then, we can retrieve a human control input pdf from the trained stochastic human behavior model using the Gaussian Mixture Regression (GMR). The proposed algorithm predicts the multi-rotor's future state pdf by propagating the pdf of the retrieved human control input according to the given dynamics, which yields closed-loop analysis of the HiLCPS. Human subject experiment results are provided to demonstrate the effectiveness of the proposed algorithm.

Keywords: Gaussian Mixture Model, Cyber Physical System, Human Model, Linear System, Human-in-the-Loop Cyber Physical System

1. INTRODUCTION

Ensuring safe operation is a crucial task to enhance the reliability of a Human-in-the-Loop Cyber Physical System (HiLCPS). To this end, there have been various approaches to assess the safety of the HiLCPS. Reachability analysis is one of the commonly applied techniques to derive the safety envelope of the system. The reachability analysis computes the set of reachable state which the HiLCPS will arrive at the specific time instant, thus it can verify if the system violates safety conditions in future. For instance, a safety guaranteeing controller which considers a human counterpart was developed based on the Hamilton-Jacobi backward reachable set in Leung et al. (2018, 2020).

Nevertheless, computing a reachable set relying on a given system dynamics may yield overly conservative reachable set (Govindarajan et al. (2017)). To address this issue, the closed-loop analysis should be performed, i.e., a human operator's behavior needs to be considered to achieve the less conservative reachable set for the HiLCPS. One can prevent the reachable set from including the states which a human operator does not tend to reach in practice by incorporating human behavioral data. However, there have been relatively few approaches that compute the reachable set based on human behavioral data. Except some existing papers (Driggs-Campbell et al. (2018); Govindarajan et al. (2017)), most of the works relied on the dynamics of a

system or a given bound of states. Even most of the stochastic reachability analysis approaches, which is beneficial for making less conservative decisions by ignoring the reachable state with negligible probability (Vinod et al. (2017)), only considered the uncertainty coming from noise or disturbance.

To address the aforementioned issue, we propose a state prediction method that can avoid the conservativeness of the existing reachability analysis by propagating probability distribution function (pdf) derived from a stochastic human behavior model as opposed to directly compute the reachable set. We select the Gaussian Mixture Model (GMM) as a basis model for the stochastic human behavior model. The GMM has been shown to be a good representation of human operators' reaction (Wang et al. (2018)). Moreover, the GMM can approximate non-Gaussian distributions (Pishdad and Labeau (2016)), thereby allowing our proposed algorithm to be extended for more general stochastic human models.

The objective of the proposed algorithm is to predict the pdf of the multi-rotor's future state in a near-collision situation. In this scenario, we assume the multi-rotor is controlled by a human operator. First, the stochastic human behavior model is trained as a GMM using the Expectation Maximization (EM) algorithm and the flight trajectory from human subject experiments. We assume the trained model represents the joint distribution between the human operator's control inputs and time, i.e., the model includes
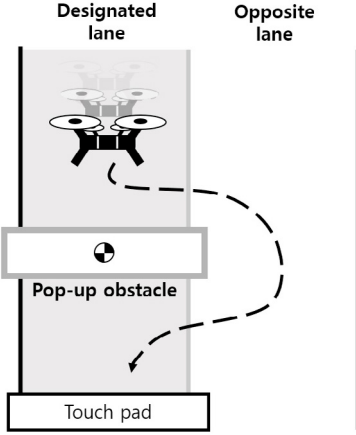
Fig. 1. Landing mission of the multi-rotor

the expected time-indexed future control input trajectory. Then, the human operator's control input pdf retrieved using the Gaussian Mixture Regression (GMR) is propagated according to the given linear dynamics. Assuming the initial uncertainty is also given as a GMM, the resulting pdf of the future state can be derived as a form of the GMM. A Gaussian mixture reduction technique is used to alleviate the computational complexity.

The contributions of this paper are as follows: (a) We propose the state prediction method that can explicitly account for the stochastic human behavior model to mitigate the conservativeness of the conventional reachable set methods. To this end, a closed-form equation is derived based on the Chapman-Kolmogorov equation that iteratively computes the pdf of the future multi-rotor state. (b) The proposed state prediction algorithm is demonstrated using the stochastic human behavior model of the multi-rotor. The stochastic human behavior model is trained using the data obtained from the human subject experiments setting on the near-collision scenario of the multi-rotor. Through the experiments, the performance of the proposed state prediction algorithm is demonstrated.

The rest of the paper is organized as follows: In Section 2, detailed information about the experiment scenario and the multi-rotor system is given. The method to train the stochastic human behavior model is introduced in Section 3. In Sections 4 and 5, the state prediction algorithm for the multi-rotor and the experiment results are presented, respectively. Lastly, conclusions are given in Section 6.

2. NEAR-COLLISION SCENARIO

Figure 1 shows a multi-rotor landing mission scenario for human subject experiments. The objective of the experiment is to extract collision avoidance reaction of a human operator in the multi-rotor system. Motivated by the existing works about rear-collision of a car (Angkititrakul et al. (2011); Luster and Pitts (2021)), we design the simulator which can observe the participants' evasive maneuver. The simulation is set on the 2-D environment with a pop-up obstacle. The participants should land the multi-rotor on a touch pad without any collision with the obstacle. In addition, the participants are asked to follow a designated lane while maintaining constant downward speed during the experiments. In each trial, the location where the obstacle
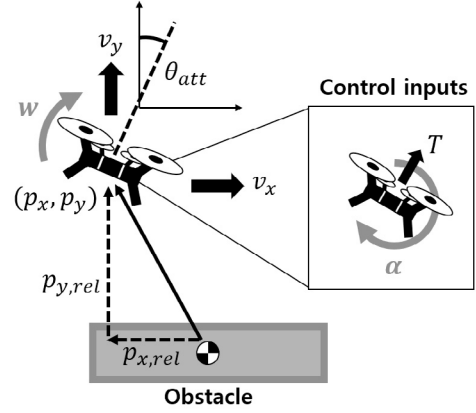

Fig. 2. State variables of the multi-rotor

pops up is not informed to the participants in advance. By focusing on the initial few seconds of the trajectory after the obstacle is spawned, we can train a stochastic human behavior model that represents the participants' collision avoidance reaction.

Figure 2 shows the state variables of the simulated multi-rotor. Based on Sabatino (2015) and Byeon et al. (2021), the linearized dynamics of the multi-rotor is modeled as

$$\boldsymbol{x}_{k+1} = A\boldsymbol{x}_k + B\boldsymbol{u}_k, \tag{1}$$

where $\boldsymbol{x}_k$ and $\boldsymbol{u}_k$ are the state and the control input vectors at time step k, respectively. Here, the state vector $\boldsymbol{x}_k \in \mathbb{R}^6$ is defined as $\boldsymbol{x}_k = [p_{x,k}, p_{y,k}, \theta_{att,k}, v_{x,k}, v_{y,k}, w_k]^T$, which consists of the position $(p_{x,k}, p_{y,k})$, the attitude $(\theta_{att,k})$, the linear velocity $(v_{x,k}, v_{y,k})$, and the angular velocity (w_k). The control input $\boldsymbol{u}_k \in \mathbb{R}^2$ is defined as $\boldsymbol{u}_k = [\alpha_k, T_k]^T$ where α and T are the angular acceleration and the thrust, respectively. A and B matrices can be written as

$$A = I_6 + \begin{pmatrix} 0 & 0 & 0 & 1 & 0 & 0 \\ 0 & 0 & 0 & 0 & 1 & 0 \\ 0 & 0 & 0 & 0 & 0 & 1 \\ 0 & 0 & g & 0 & 0 & 0 \\ 0 & 0 & 0 & 0 & k_1 & 0 \\ 0 & 0 & k_2 & 0 & 0 & k_3 \end{pmatrix} \Delta t, \tag{2}$$

$$B = \begin{pmatrix} 0 & 0 \\ 0 & 0 \\ 0 & 0 \\ 0 & 0 \\ 0 & 1/m \\ 1/I_x & 0 \end{pmatrix} \Delta t, \tag{3}$$

where Δt is the discretization time interval, g is the gravitational acceleration, m and I_x are the mass and the moment of inertial of the multi-rotor, respectively, k_1, k_2, and k_3 are the controller parameters, and I_6 is the 6×6 identity matrix. A and B are computed by linearizing the multi-rotor's dynamics with respect to a hovering point (Sabatino (2015)).

3. STOCHASTIC HUMAN BEHAVIOR MODEL

In this section, we train the stochastic human behavior model using the data collected from the human subject experiments. Using the Expectation Maximization (EM) algorithm, we can compute the stochastic human behavior

model which contains the joint distribution between the participants' control input and the time elapsed after the obstacle is spawned. The trained stochastic human behavior model will be utilized as the prior knowledge for the multi-rotor's state prediction in Section 4.

The GMM is a combination of multiple Gaussian distributions. Assuming a distribution of state x follows the GMM, the pdf of x, $P(x)$, is defined as

$$P(x) = \sum_{i=1}^{M} \pi_i N(\mu_i, \Sigma_i), \qquad (4)$$

where π_i is the weight of each Gaussian component satisfying $\sum_{i=1}^{M} \pi_i = 1$ and $N(\mu_i, \Sigma_i)$ is the Gaussian distribution which has μ_i and Σ_i as the mean and the covariance, respectively. In this paper, we focus on the joint distribution between the human control input and time, which can be represented as a GMM. Accordingly, the trajectory used to train the stochastic human behavior model is written as $\boldsymbol{\zeta} = [\boldsymbol{\zeta}_0^T, \boldsymbol{\zeta}_1^T, \cdots, \boldsymbol{\zeta}_{t_f}^T]^T$ where $\boldsymbol{\zeta}_k = [t_k, \boldsymbol{u}_k^T]^T$, $t_k = k\Delta t$, and t_f is the end time of the trajectory. It is worth noting that t_0 is the time when the obstacle is spawned. The proper parameters of the stochastic human behavior model can be computed by feeding $\boldsymbol{\zeta}$ to the EM algorithm. The trained stochastic human behavior model can be expressed as (Calinon (2016))

$$P(\boldsymbol{u}, \boldsymbol{t}) = \sum_{i=1}^{M} \pi_{p,i} N(\boldsymbol{\mu}_{p,i}, \boldsymbol{\Sigma}_{p,i}), \qquad (5)$$

where $\boldsymbol{u} = [\boldsymbol{u}_1^T, \boldsymbol{u}_2^T, \cdots, \boldsymbol{u}_{t_f}^T]^T$, $\boldsymbol{t} = [t_1, t_2, \cdots, t_{t_f}]^T$, and $\pi_{p,i}$, $\boldsymbol{\mu}_{p,i}$, and $\boldsymbol{\Sigma}_{p,i}$ are the weight, mean, and covariance matrix for each Gaussian component, respectively. The EM algorithm finds the value of each Gaussian component's parameters ($\pi_{p,i}$, $\boldsymbol{\mu}_{p,i}$, and $\boldsymbol{\Sigma}_{p,i}$) which are the best fit for representing the given trajectory. Throughout the paper, we assume that the stochastic human behavior model is composed of M number of Gaussian components, which is a design parameter, and properly trained through sufficient amount of data thereby it well represents the human operators' evasive behavior.

4. STATE PREDICTION OF MULTI-ROTOR

4.1 State prediction based on stochastic human behavior model

The Gaussian Mixture Regression (GMR) allows us to retrieve the conditional distribution of the human control input at a given time instant (Calinon (2016); Stulp and Sigaud (2015)). From (5), let $\boldsymbol{\mu}_{p,i}$ and $\boldsymbol{\Sigma}_{p,i}$ be defined as

$$\boldsymbol{\mu}_{p,i} = \begin{pmatrix} \boldsymbol{\mu}_{p,i}^u \\ \boldsymbol{\mu}_{p,i}^t \end{pmatrix}, \boldsymbol{\Sigma}_{p,i} = \begin{pmatrix} \boldsymbol{\Sigma}_{p,i}^u & \boldsymbol{\Sigma}_{p,i}^{ut} \\ \boldsymbol{\Sigma}_{p,i}^{tu} & \boldsymbol{\Sigma}_{p,i}^t \end{pmatrix}. \qquad (6)$$

In (6), $\boldsymbol{\mu}_{p,i}^u \in \mathbb{R}^2$ is the mean fraction corresponding to the human control input, $\boldsymbol{\mu}_{p,i}^t \in \mathbb{R}$ is that of time, and $\boldsymbol{\Sigma}_{p,i}^u$, $\boldsymbol{\Sigma}_{p,i}^t$, $\boldsymbol{\Sigma}_{p,i}^{ut}$, and $\boldsymbol{\Sigma}_{p,i}^{tu}$ are the corresponding covariance fractions, respectively. Then, the conditional distribution of the human input at time step k is (Calinon (2016))

$$P(\boldsymbol{u}|t_k) = P(\boldsymbol{u}_k) = \sum_{i=1}^{M} \hat{\pi}_{p,i}(t_k) N(\hat{\boldsymbol{\mu}}_{p,i}(t_k), \hat{\boldsymbol{\Sigma}}_{p,i}), \qquad (7)$$

where

$$\hat{\boldsymbol{\mu}}_{p,i}(t_k) = \boldsymbol{\mu}_{p,i}^u + \boldsymbol{\Sigma}_{p,i}^{ut} \boldsymbol{\Sigma}_{p,i}^{t^{-1}} (t_k - \boldsymbol{\mu}_{p,i}^t), \qquad (8)$$

$$\hat{\boldsymbol{\Sigma}}_{p,i} = \boldsymbol{\Sigma}_{p,i}^u - \boldsymbol{\Sigma}_{p,i}^{ut} \boldsymbol{\Sigma}_{p,i}^{t^{-1}} \boldsymbol{\Sigma}_{p,i}^{tu}, \qquad (9)$$

$$\hat{\pi}_{p,i}(t_k) = \frac{\pi_{p,i} N(t_k|\boldsymbol{\mu}_{p,i}^t, \boldsymbol{\Sigma}_{p,i}^t)}{\sum_{j}^{M} \pi_{p,j} N(t_k|\boldsymbol{\mu}_{p,j}^t, \boldsymbol{\Sigma}_{p,j}^t)}. \qquad (10)$$

Our objective is to compute the pdf of the future state at time step $k + T$, $P(x_{k+T})$, using the human operator's evasive behavior information achieved in (7). Assume that the current state ($\boldsymbol{x}_k$) has uncertainty represented as a GMM with L Gaussian components:

$$\boldsymbol{x}_k \sim \sum_{i=1}^{L} \pi_{\boldsymbol{x}_k,i} N(\boldsymbol{\mu}_{\boldsymbol{x}_k,i}, \boldsymbol{\Sigma}_{\boldsymbol{x}_k,i}) \qquad (11)$$

The propagation of the state pdf can be computed by Chapman–Kolmogorov equation.

$$P(\boldsymbol{x}_{k+1}) = \int_{\boldsymbol{x}_k} P(\boldsymbol{x}_{k+1}|\boldsymbol{x}_k) P(\boldsymbol{x}_k) d\boldsymbol{x}_k \qquad (12)$$

From (12), using the dynamics (1) and the input pdf (7), $P(\boldsymbol{x}_{k+1}|\boldsymbol{x}_k)$ can be rewritten as:

$$P(\boldsymbol{x}_{k+1}|\boldsymbol{x}_k) = \sum_{i=1}^{M} \hat{\pi}_{p,i}(t_k) N(A\boldsymbol{x}_k + B\hat{\boldsymbol{\mu}}_{p,i}(t_k), B\hat{\boldsymbol{\Sigma}}_{p,i} B^T) \qquad (13)$$

By substituting equation (13) for $P(\boldsymbol{x}_{k+1}|\boldsymbol{x}_k)$ in (12), we obtain

$$P(\boldsymbol{x}_{k+1}) =$$
$$\int_{\boldsymbol{x}_k} \sum_{i=1}^{M} \hat{\pi}_{p,i}(t_k) N(A\boldsymbol{x}_k + B\hat{\boldsymbol{\mu}}_{p,i}(t_k), B\hat{\boldsymbol{\Sigma}}_{p,i} B^T) P(\boldsymbol{x}_k) d\boldsymbol{x}_k, \qquad (14)$$

and if we replace $P(\boldsymbol{x}_k)$ with (11), we have

$$P(\boldsymbol{x}_{k+1}) =$$
$$\int_{\boldsymbol{x}_k} \sum_{i=1}^{M} \hat{\pi}_{p,i}(t_k) N(A\boldsymbol{x}_k + B\hat{\boldsymbol{\mu}}_{p,i}(t_k), B\hat{\boldsymbol{\Sigma}}_{p,i} B^T) \cdot$$
$$\sum_{j=1}^{L} \pi_{\boldsymbol{x}_k,j} N(\boldsymbol{\mu}_{\boldsymbol{x}_k,j}, \boldsymbol{\Sigma}_{\boldsymbol{x}_k,j}) d\boldsymbol{x}_k. \qquad (15)$$

By Karumanchi and Tulpule (2021), equation (15) can be rewritten as a GMM with ML number of Gaussian components:

$$P(\boldsymbol{x}_{k+1}) = \frac{1}{\eta} \sum_{i=1}^{M} \hat{\pi}_{p,i}(t_k) \sum_{j=1}^{L} \pi_{\boldsymbol{x}_k,j} \cdot$$
$$N(A\boldsymbol{\mu}_{\boldsymbol{x}_k,j} + B\hat{\boldsymbol{\mu}}_{p,i}(t_k), B\hat{\boldsymbol{\Sigma}}_{p,i} B^T + A\boldsymbol{\Sigma}_{\boldsymbol{x}_k,j} A^T), \qquad (16)$$

where η is a normalization constant to ensure the integral of (16) is 1.

One can compute $P(\boldsymbol{x}_{k+T})$ by repeating (11)-(16) to time step T. However, this process is computationally demanding as the number of Gaussian components grows rapidly. For each time step, it increases by M times since we assume the stochastic human behavior model is composed of M Gaussian components.

4.2 Gaussian mixture reduction

As shown in the previous section, the combination of GMMs leads to the rapid growth of the number of Gaussian components. To address this issue, there have been various studies to efficiently reduce the number of Gaussian components (Zhang and Chen (2020)). One of the methods is using the Kullback-Leibler (K-L) divergence, which represents the difference between two distributions. Unfortunately, the closed form of the K-L divergence between two GMMs is known to be unavailable. To tackle this problem, a novel reduction algorithm was proposed in Runnalls (2007) based on the upper bound of the K-L divergence.

Let $\hat{P}(\boldsymbol{x}_{k+1})$ be the reduced GMM from $P(\boldsymbol{x}_{k+1})$ by merging the Gaussian components i and j into a single Gaussian. The author merged the pair which induces the lowest upper bound of the K-L divergence between $\hat{P}(\boldsymbol{x}_{k+1})$ and $P(\boldsymbol{x}_{k+1})$. We adopt this approach to reduce the number of Gaussian components. Let $(\boldsymbol{\Sigma}_i, \boldsymbol{\Sigma}_j)$ be a pair of the covariance matrices of the selected Gaussian components from $P(\boldsymbol{x}_{k+1})$. (π_i, π_j) and $(\boldsymbol{\mu}_i, \boldsymbol{\mu}_j)$ are the corresponding weights and means. The merged covariance $\boldsymbol{\Sigma}_{ij}$ can be computed as

$$\boldsymbol{\Sigma}_{ij} = \frac{\pi_i}{\pi_i + \pi_j}\boldsymbol{\Sigma}_i + \frac{\pi_j}{\pi_i + \pi_j}\boldsymbol{\Sigma}_j + \frac{\pi_i \pi_j}{(\pi_i + \pi_j)^2}(\boldsymbol{\mu}_i - \boldsymbol{\mu}_j)(\boldsymbol{\mu}_i - \boldsymbol{\mu}_j)^T. \quad (17)$$

From (17), the upper bound of the K-L divergence $(KL_{up}(i,j))$ is defined as follow:

$$KL_{up}(i,j) = \frac{1}{2}[(\pi_i + \pi_j)ln(det(\boldsymbol{\Sigma}_{ij})) - \pi_i ln(det(\boldsymbol{\Sigma}_i)) - \pi_j ln(det(\boldsymbol{\Sigma}_j))] \quad (18)$$

Then, the pair (i,j) with the minimum KL_{up} is merged into a single Gaussian, $\pi_{ij}N(\boldsymbol{\mu}_{ij}, \boldsymbol{\Sigma}_{ij})$, where $\pi_{ij} = \pi_i + \pi_j$ and $\boldsymbol{\mu}_{ij} = \frac{\pi_i}{\pi_{ij}}\boldsymbol{\mu}_i + \frac{\pi_j}{\pi_{ij}}\boldsymbol{\mu}_j$ (Runnalls (2007)). As a result, one can maintain the number of Gaussian components by repeating the above process until it reaches the desired number.

5. EXPERIMENT SETUP AND RESULT

5.1 Stochastic human behavior model training

We first train the stochastic human behavior model using the data obtained from the human subject experiments. A total of 11 participants are recruited from Purdue University [1]. Among the collected data, initial 4.5 [s] of the trajectory after the obstacle spawned is extracted from each successful landing trial. It yields total 544.5 [s] of training data from 121 trials. We separate a single trial (4.5 [s]) as validation data and set $M = 3$ for the EM algorithm.

Figure 3 shows the randomly selected 10 flight logs and the GMR result for the initial 4.5 [s] after the obstacle spawned. The green line describes the mean of the GMR
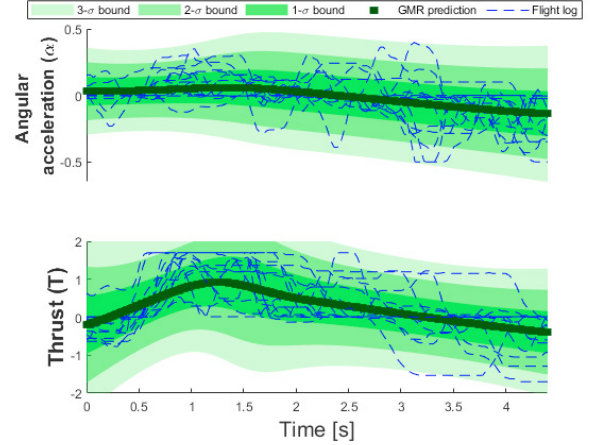
Fig. 3. GMR prediction of human control input

Table 1. Simulation parameters

Discretization time interval (Δt)	$0.04\ [s]$
Gravitational acceleration (g)	$9.8\ [m/s^2]$
Mass (m)	$0.25\ [kg]$
Moment of inertia (I_x)	$0.01\ [kg \cdot m^2]$
Control parameter (k_1, k_2, k_3)	$-0.1, -1, -30$
Thrust input bound (T)	$[-1.7, 1.7]$
Angular acceleration input bound (α)	$[-0.5, 0.5]$
Maximum Gaussian components	16

result while blue lines are the participants' control input logs. The green shaded regions represent the 1, 2, and 3-σ bound of the GMR result, respectively, where σ is the standard deviation. As shown in the figure, the trained model successfully predicts the participants' input within 2-σ bound most of the time.

5.2 State prediction result

In this subsection, the state prediction results of the proposed algorithm are presented. Starting from t_0, the proposed algorithm predicts the states of the multi-rotor at 1.5, 3, and 4 [s]. Moreover, the comparison with Monte-Carlo simulation of 5000 samples is also provided to demonstrate the effectiveness of the proposed algorithm. Table 1 shows the parameters used for the simulation. In the simulation, we assume that the initial state has uncertainty represented as a GMM with three Gaussian components. Accordingly, the initial state, $\boldsymbol{x}_0 = [p_{x,0}, p_{y,0}, \theta_{att,0}, v_{x,0}, v_{y,0}, w_0]^T$, with the GMM uncertainty can be written as

$$\bar{\boldsymbol{x}}_0 = \boldsymbol{x}_0 + \sum_{i=1}^{M} \pi_{c,i} N(\boldsymbol{\mu}_{c,i}, \boldsymbol{\Sigma}_{c,i}), \quad (19)$$

where $\pi_{c,1} = \pi_{c,2} = \pi_{c,3} = \frac{1}{3}$, $\boldsymbol{\Sigma}_{c,1}$, $\boldsymbol{\Sigma}_{c,2}$, and $\boldsymbol{\Sigma}_{c,3}$ are identical matrices whose diagonal components are $diag[1.5, 1.5, 0.05, 1, 2, 0.05]$ and 0 elsewhere, and

$$\boldsymbol{\mu}_{c,1} = [0, 0, 0, 0, 0, 0]^T,$$
$$\boldsymbol{\mu}_{c,2} = [1, 1, 0.1, 1, 1, 0.05]^T, \quad (20)$$
$$\boldsymbol{\mu}_{c,3} = [-1, 1, -0.1, -1, -1, -0.05]^T.$$

The initial state of each Monte-Carlo simulation is sampled from (19) and propagates through the dynamics (1). We assume the control inputs (α, T) are uniformly distributed
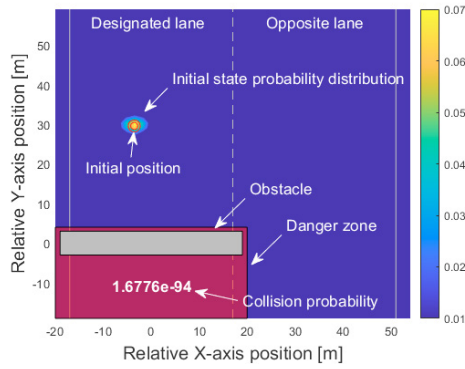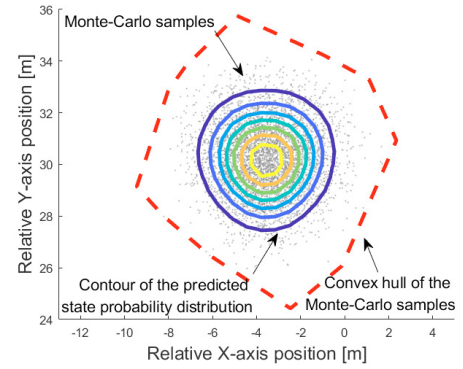
(a) $T = 0\ [s]$, with initial uncertainty

(b) $T = 1.5\ [s]$
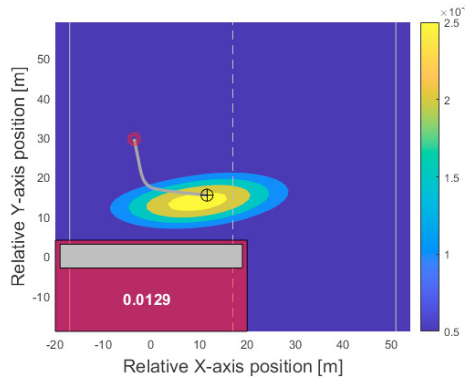
(c) $T = 3\ [s]$
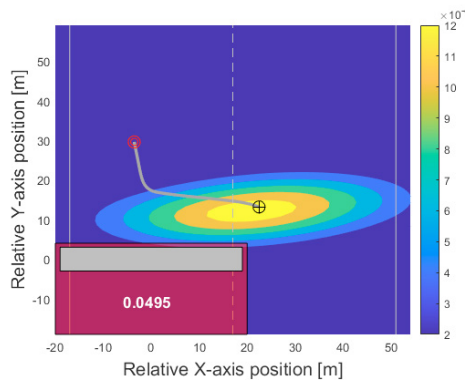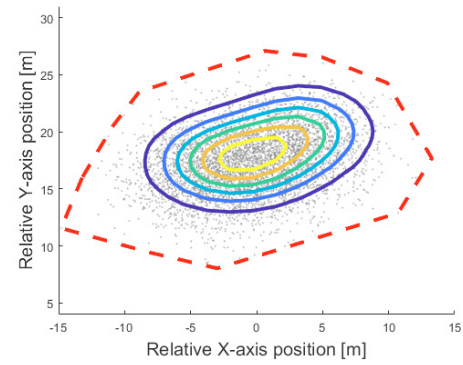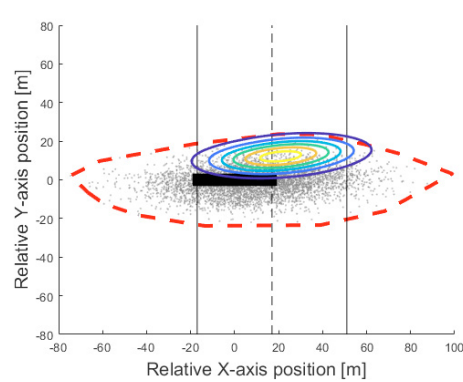
(d) $T = 4\ [s]$

Fig. 4. Comparison between the predicted probability distribution and the true trajectory

(a) $T = 0\ [s]$

(b) $T = 1.5\ [s]$

(c) $T = 3\ [s]$

(d) $T = 4\ [s]$

Fig. 5. Comparison between the Monte-Carlo simulation and the proposed state prediction algorithm

with the bound $\alpha \in [-0.5, 0.5]$ and $T \in [-1.7, 1.7]$ for the Monte-Carlo simulation, as shown in Table 1.

Figure 4 shows the state prediction result at each specific time instant. In the figures, the grey box is the obstacle, the red circle is the initial position, the grey line is the actual trajectory of the multi-rotor, and the black circle is the position of the multi-rotor at the given time instant. The white lines at each side of the figures and the dotted line at the center divide the lanes, which are described in Fig. 1. The red box at the bottom of the figures is the danger zone where the multi-rotor should avoid. The collision probability is obtained by computing the cumulative probability of the predicted pdf on the danger zone. Figure 4a describes the initial state with the uncertainty given in (20). Meanwhile, Figs. 4b-4d represent the predicted state pdf at each time instant. The brighter area means higher probability. Due to the initial uncertainty and the stochastic human behavior model, the pdf expands over time. Nevertheless, the additional probabilistic information gives more weight on a certain area unlike the conventional reachable set.

Figures 5a-5d are the comparison between the proposed algorithm and the Monte-Carlo simulation. The contour describes the predicted pdf, the grey dots are the Monte-Carlo samples, and the red dotted line is the convex hull of the samples. The black lines and box represent the lanes and the obstacle, respectively. In the figures, the resulting contour significantly reduces the area that the multi-rotor is likely to reach in comparison with the convex hull. This advantage is clearly shown in 3-4 $[s]$. In Figs. 5c-5d, the Monte-Carlo samples indicate that the multi-rotor can reach the obstacle although there was no collision during the flight. In contrast, the proposed approach shows in Figs. 4c-4d that the multi-rotor is not likely to collide, thereby alleviating the conservativeness of reachable states, a well-known weakness of the reachability analysis.

6. CONCLUSION

In this paper, we proposed the state prediction algorithm for the Human-in-the-Loop Cyber Physical System (HiLCPS) which explicitly considers the stochastic human behavior model. The proposed algorithm computes the state pdf of the multi-rotor at a desired future time instant. The computed pdf provides probabilistic information that can be facilitated for safe controller design compared to a simple set of states which further improves the reliability of the system.

For future work, the human behavior model which represents the joint distribution between vehicle states and human control inputs will be examined. We expect that the human model which includes a vehicle's state can express more general and complex human action, therefore improve the prediction accuracy of the proposed algorithm.

REFERENCES

Angkititrakul, P., Miyajima, C., and Takeda, K. (2011). Modeling and adaptation of stochastic driver-behavior model with application to car following. In *2011 IEEE Intelligent Vehicles Symposium (IV)*, 814–819.

Byeon, S., Sun, D., and Hwang, I. (2021). Skill-level-based hybrid shared control for human-automation systems. In *2021 IEEE International Conference on Systems, Man, and Cybernetics (SMC)*, 1507–1512.

Calinon, S. (2016). A tutorial on task-parameterized movement learning and retrieval. *Intelligent Service Robotics*, 9(1), 1–29.

Driggs-Campbell, K., Dong, R., and Bajcsy, R. (2018). Robust, informative human-in-the-loop predictions via empirical reachable sets. *IEEE Transactions on Intelligent Vehicles*, 3(3), 300–309.

Govindarajan, V., Driggs-Campbell, K., and Bajcsy, R. (2017). Data-driven reachability analysis for human-in-the-loop systems. In *2017 IEEE 56th Annual Conference on Decision and Control (CDC)*, 2617–2622.

Karumanchi, A. and Tulpule, P. (2021). Comparing linear systems with Gaussian mixture model additive uncertainties using Kullback-Leibler rate. *IFAC-PapersOnLine*, 54(20), 566–572.

Leung, K., Schmerling, E., Chen, M., Talbot, J., Gerdes, J.C., and Pavone, M. (2018). On infusing reachability-based safety assurance within probabilistic planning frameworks for human-robot vehicle interactions. In *International Symposium on Experimental Robotics*, 561–574. Springer.

Leung, K., Schmerling, E., Zhang, M., Chen, M., Talbot, J., Gerdes, J.C., and Pavone, M. (2020). On infusing reachability-based safety assurance within planning frameworks for human–robot vehicle interactions. *The International Journal of Robotics Research*, 39(10-11), 1326–1345.

Luster, M.S. and Pitts, B.J. (2021). A preliminary investigation into learning behaviors in complex environments for human-in-the-loop cyber-physical systems. In *Proceedings of the Human Factors and Ergonomics Society Annual Meeting*, 1, 42–46.

Pishdad, L. and Labeau, F. (2016). Approximate MMSE estimator for linear dynamic systems with Gaussian mixture noise. *IEEE Transactions on Automatic Control*, 62(5), 2457–2463.

Runnalls, A.R. (2007). Kullback-Leibler approach to Gaussian mixture reduction. *IEEE Transactions on Aerospace and Electronic Systems*, 43(3), 989–999.

Sabatino, F. (2015). Quadrotor control: modeling, nonlinear control design, and simulation. *Master thesis, KTH Royal Institute of Technology*.

Stulp, F. and Sigaud, O. (2015). Many regression algorithms, one unified model: A review. *Neural Networks*, 69, 60–79.

Vinod, A.P., HomChaudhuri, B., and Oishi, M.M. (2017). Forward stochastic reachability analysis for uncontrolled linear systems using Fourier transforms. In *Proceedings of the 20th International Conference on Hybrid Systems: Computation and Control*, 35–44.

Wang, W., Xi, J., and Zhao, D. (2018). Learning and inferring a driver's braking action in car-following scenarios. *IEEE Transactions on Vehicular Technology*, 67(5), 3887–3899.

Zhang, Q. and Chen, J. (2020). A unified framework for Gaussian mixture reduction with composite transportation distance. *arXiv Preprint arXiv:2002.08410*.